

# Interferon- $\gamma$ -mediated Inhibition of Serum Response Factor-dependent Smooth Muscle-specific Gene Expression<sup>\*[S]</sup>

Received for publication, July 20, 2010, and in revised form, July 30, 2010. Published, JBC Papers in Press, August 4, 2010, DOI 10.1074/jbc.M110.164863

Zengdun Shi and Don C. Rockey<sup>1</sup>

From the Department of Internal Medicine, Division of Digestive and Liver Diseases, University of Texas Southwestern Medical Center at Dallas, Dallas, Texas 75390

IFN $\gamma$  exerts multiple biological effects on effector cells by regulating many downstream genes, including smooth muscle-specific genes. However, the molecular mechanisms underlying IFN $\gamma$ -induced inhibition of smooth muscle-specific gene expression remain unclear. In this study, we have shown that serum response factor (SRF), a common transcriptional factor important in cell proliferation, migration, and differentiation, is targeted by IFN $\gamma$  in a STAT1-dependent manner. We show that the molecular mechanism by which IFN $\gamma$  regulates SRF is via activation of the 2-5A-RNase L system, which triggers SRF mRNA decay and reduced SRF expression. As a result, decreased SRF expression reduces expression of SRF target genes such as smooth muscle  $\alpha$ -actin and smooth muscle myosin heavy chain. Additionally, IFN $\gamma$  reduced p300 and acetylated histone-3 binding in both smooth muscle  $\alpha$ -actin and SRF promoters, epigenetically decreasing smooth muscle  $\alpha$ -actin and SRF transcriptional activation. Our data reveal that SRF is a novel IFN $\gamma$ -regulated gene and further elucidate the molecular pathway between IFN $\gamma$ , IFN $\gamma$ -regulated genes, and SRF and its target genes.

IFN $\gamma$ , a pleiotropic cytokine that is primarily produced by T cells and NK cells, plays a complex and central role in antiviral, antiproliferative, antifibrogenesis, antitumor, and immunomodulatory activities (reviewed in Refs. 1 and 2). The complexity of such a variety of IFN $\gamma$  effects appears to be achieved by its signaling to over 200 genes, leading to a highly networked pattern of cell-specific gene regulation (3). In the canonical pathway, through binding to cognate IFN type II receptors, IFN $\gamma$  initiates a cascade that includes JAK family kinases and the STAT1 family of transcriptional factors to induce STAT1-dependent gene expression, which largely mediates the actions of IFN $\gamma$  (reviewed in Ref. 4). Among IFN $\gamma$ -regulated genes, smooth muscle  $\alpha$ -actin, a cytoskeleton protein that is critical in smooth muscle cell differentiation (reviewed in Ref. 5), myofibroblast activation (reviewed in Ref. 6), and epithelial-mesenchymal transition (7), is negatively regulated by IFN $\gamma$  (8, 9). Although the observation that IFN $\gamma$  regulates smooth muscle

$\alpha$ -actin is well established, the molecular mechanisms underlying IFN $\gamma$ -induced inhibition of smooth muscle  $\alpha$ -actin expression remain unclear.

Regulation of smooth muscle  $\alpha$ -actin expression is complex, having been studied extensively in cardiovascular and vascular diseases, particularly in smooth muscle cells (reviewed in Ref. 5). It has been well demonstrated that most muscle-specific genes, including smooth muscle  $\alpha$ -actin, are SRF<sup>2</sup> target genes. SRF binds to the CArG boxes (CC(A/T)<sub>6</sub>GG) of the smooth muscle  $\alpha$ -actin gene promoter and activates smooth muscle  $\alpha$ -actin transcription (reviewed in Ref. 10). Extracellular factors can exert their effects on smooth muscle gene expression through regulating SRF or/and SRF cofactors (11). TGF $\beta$ , a well characterized cytokine important in smooth muscle cell differentiation and epithelial-mesenchymal transition, up-regulates smooth muscle  $\alpha$ -actin expression in both smooth muscle and nonsmooth muscle cells and is mediated through a TGF $\beta$ -responsive element in smooth muscle  $\alpha$ -actin gene promoter (12) and elevation of SRF expression (13, 14). Although IFN $\gamma$  clearly exhibits an inhibitory effect on smooth muscle  $\alpha$ -actin expression in smooth muscle (8) and nonsmooth muscle cell types (9), its effects on the smooth muscle  $\alpha$ -actin promoter are unknown.

Previous studies have shown that IFN $\gamma$  inhibits smooth muscle  $\alpha$ -actin expression in activated hepatic stellate cells (9), a cell type that undergoes phenotypic transition to a myofibroblast-like cell in a process that is tightly linked to a smooth muscle-specific gene expression program (15, 16). Further, IFN $\gamma$  exerts a protective role in liver fibrogenesis, likely via effects on stellate cells (17). In the present study, we have demonstrated the presence of a novel signaling network linking IFN $\gamma$ , SRF, and smooth muscle-specific genes. We show that the mechanism by which IFN $\gamma$  regulates SRF is via the 2-5A-RNase L system, which triggers SRF mRNA decay. The degradation of SRF mRNA, in turn, creates a negative autoregulatory cycle, which further reduces SRF expression (18) and consequently reduces smooth muscle  $\alpha$ -actin and smooth muscle myosin heavy chain (SMMHC). The findings provide novel insight into the molecular mechanism of IFN $\gamma$ -mediated regulation of smooth muscle-specific genes.

\* This work was supported, in whole or in part, by National Institutes of Health Grants R01 DK 60338 and R01 DK 50574 (to D. C. R.).

[S] The on-line version of this article (available at <http://www.jbc.org>) contains supplemental text, Table S1, and Figs. S1–S3.

<sup>1</sup> To whom correspondence should be addressed: Division of Digestive and Liver Diseases, University of Texas Southwestern Medical Center, 5323 Harry Hines Blvd., Dallas, TX 75390-8887. Tel.: 214-648-3444; Fax: 214-648-0274; E-mail: don.rockey@utsouthwestern.edu.

<sup>2</sup> The abbreviations used are: SRF, serum response factor; SM  $\alpha$ -actin, smooth muscle  $\alpha$ -actin; H3Ac, acetylated histone 3; SMMHC, smooth muscle myosin heavy chain; RPA, RNase protection assay; MEF, mouse embryo fibroblast; GAS,  $\gamma$ -activated site(s); 2-5A, 2'-5'-phosphodiester-linked oligoadenylates.

### EXPERIMENTAL PROCEDURES

**Stellate Cell Isolation, Culture, and Animals**—All stellate cells used in the experiments presented were primary cells isolated from normal Sprague-Dawley rats or wild type Balb/c or STAT1-deficient mice as described in the [supplemental data](#). STAT1-deficient mice (129S6/SvEV; Taconic Farms, Germantown, NY) were backcrossed with Balb/c inbred mice (Taconic) for more than four generations. Genotyping of the mice was performed by PCR as described (17). Cell purity was assessed by examination of morphologic features, vitamin A droplets, and immunohistochemical detection of desmin (characteristic of stellate cells) and was greater than 95% pure in all cases as described previously (15). Stellate cells were cultured for 4–5 days (activated stellate cells) before experiments unless indicated otherwise. The animals were cared for and experiments were performed in accordance with National Institutes of Health guidelines.

**Plasmids**—A  $-125 + 5$ -bp fragment of the rat smooth muscle (SM)  $\alpha$ -actin promoter (SMpro-125) and a  $-787 + 11$ -bp fragment of the mouse SRF promoter (SRFpro-787) were cloned from genomic DNA using PCR. PCR primers were designed based on available DNA sequences (GenBank<sup>TM</sup> accession numbers S76011 and AC165445). The sequence of the isolated mouse SRF gene promoter (798 bp) has been submitted to GenBank<sup>TM</sup> (accession number EF654102). PCR products were ligated into a pGL3 Basic luciferase reporter vector (Promega), and a series of deletions and mutations were generated. A rat SRF mRNA 3'-UTR fragment (1,500 bp from the stop codon; GenBank<sup>TM</sup> accession number XM-576514) was cloned from rat stellate cell cDNA and inserted into the XbaI site of pGL3 promoter luciferase reporter vector. Mouse RNase L (GenBank<sup>TM</sup> accession number NM-0118820) cDNAs were cloned into a pcDNA3.1 vector (with a FLAG tag). The SMMHC promoter construct was obtained from Dr. White (University of Vermont).

For RPA cRNA probe constructs, 237-bp fragments of rat and mouse SM  $\alpha$ -actin were subcloned from SM  $\alpha$ -actin full-length cDNA (GenBank<sup>TM</sup> accession numbers X06801 and X13297, respectively) into pGEM7Zf(+) (Promega); the rat SMMHC cRNA probe was constructed by cloning a 552-bp cDNA fragment (GenBank<sup>TM</sup> accession number XM001053402) into PCRII vector (Invitrogen); a 156-bp fragment of rat SRF cDNA (GenBank<sup>TM</sup> accession number XM-576514) was cloned and ligated into pGEM7Zf(+); and a 292-bp fragment of mouse RNase L cDNA was subcloned from full-length RNase L cDNA and inserted into the XbaI and HindIII sites of pGEM7Zf(+) vector (Promega).

The sequences for the all of the constructs were confirmed by sequencing (University of Texas Southwestern DNA sequencing core facility). All of the PCR primers are available in the [supplemental data](#).

**Transfection and Luciferase Assay**—Stellate cells were transfected with 2  $\mu$ g of plasmid DNA using Lipofectamine 2000 (Invitrogen). The cells were incubated with 199OR medium containing 0.1% serum with or without IFN $\gamma$  (1,000 IU/ml; PBL Biomedical) for 2 days, and whole cell lysates were assayed using a dual-luciferase reporter assay system (Promega). All of

the transfection experiments were performed in triplicate and repeated at least three times. The number of relative light units from pGL3 basic luciferase reporter vector (pGL3B) (Promega) was arbitrarily set to 1, and the experimental data were presented as fold increase relative to pGL3B activity. The number of relative light units from pGL3 promoter-SRF mRNA 3'-UTR construct was arbitrarily set to 100, and the experimental data were presented as a percentage of decrease.

**Overexpression of Exogenous RNase L**—HEK293 cells were grown in DMEM, 10% FBS, and the expression plasmid harboring FLAG-tagged RNase L was transduced using Lipofectamine 2000 (Invitrogen) with low serum (0.5%) medium overnight. The cells were harvested after 24 h for immunoblot. Wild type RNase L (RNase L<sup>+/+</sup>) and RNase L null (RNase L<sup>-/-</sup>) mouse embryo fibroblasts (MEFs) were obtained from Dr. Silverman (Cleveland, Ohio).

**Immunoblot**—Cultured stellate cells were washed three times with cold PBS, and proteins were extracted with radioimmune precipitation assay buffer containing protease inhibitors (Roche Applied Science). The cell lysates were incubated on ice for 30 min and centrifuged at 4 °C for 20 min. The supernatant was harvested, and protein concentration was measured (Bio-Rad). Proteins were subjected to immunoblotting as described previously (19). Anti-SM  $\alpha$ -actin, anti- $\beta$ -actin, anti-FLAG M2, and anti- $\alpha$ -tubulin were from Sigma; anti-SRF and anti-pSTAT1 were from Santa Cruz, and anti-STAT1 was from BD Transduction Laboratories. Specific signals were visualized using enhanced chemiluminescence (Pierce) and captured with a digital imaging system (Chemigenius 2 photo documentation system; Syngene). The intensities of specific bands were quantified using standard software (Gene Tool, Syngene), and the raw volume from the first control sample (IFN $\gamma$  -) in each experiment was arbitrarily set at 100. The specific protein expression in each sample was presented as a percentage of decrease.

**RNase Protection Assay**—Total RNA was extracted using TRIzol (Invitrogen) and hybridized with radioactively labeled cRNA probes using an RPA III kit (Ambion) as performed (17). For RNA decay assay, stellate cells were starved (0.1% serum) for 1 day and incubated with IFN $\gamma$  (1,000 IU/ml) for 2 h, and actinomycin D (10  $\mu$ g/ml; Sigma) was subsequently added. The specific mRNA abundances at the indicated time points were measured by RPA. The raw volume from the first control sample (IFN $\gamma$  -) or actinomycin D zero time point sample was arbitrarily set at 100. The reduction of mRNA expression in each sample was presented as a percentage of decrease.

**EMSA**—Nuclear extracts were prepared as described (19). The nuclear proteins were incubated with <sup>32</sup>P-labeled double-stranded DNA probe for 30 min. The resulting DNA-protein complexes were separated by nondenaturing electrophoresis. For supershift assay, 2  $\mu$ l of anti-SRF or pSTAT1 (Santa Cruz) antibody was incubated with the reaction mixture for 30 min before incubation with <sup>32</sup>P-labeled probe. All of the oligonucleotide sequences for EMSA are available in the [supplemental data](#).

**ChIP Assay**—Stellate cells were starved (0.1% serum) for 1 day, and IFN $\gamma$  (1,000 IU/ml) was added for 16 h. ChIP assay was performed using ChIP assay kit (Upstate) as described (20). The

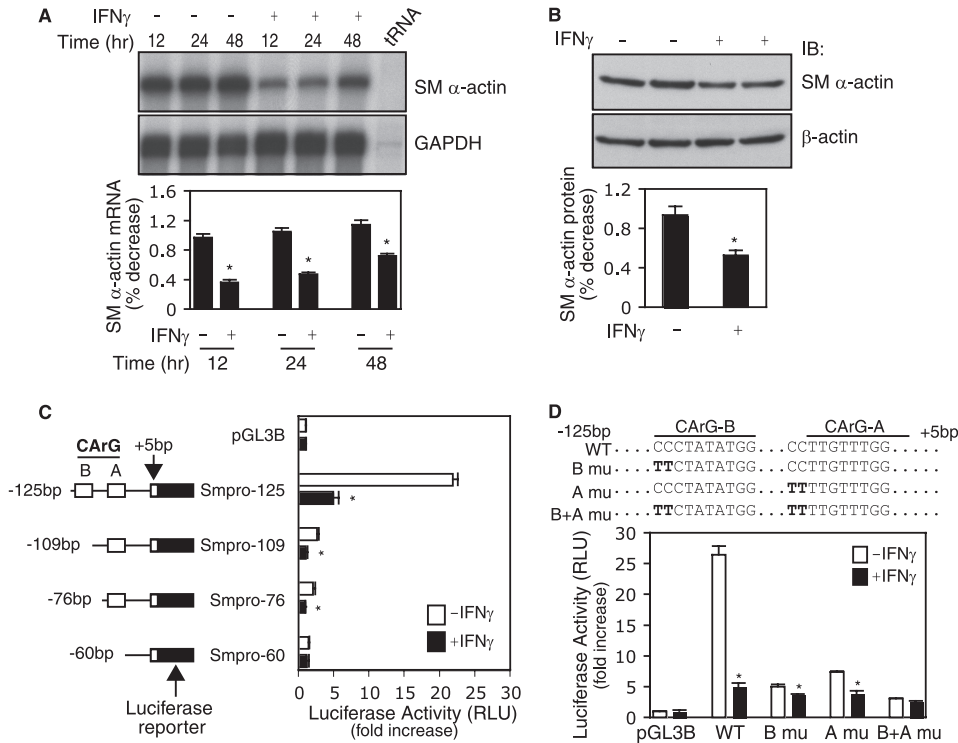


**FIGURE 1. IFN $\gamma$ -mediated inhibition of smooth muscle  $\alpha$ -actin requires CARG boxes.** A and B, stellate cells were starved (0.1% serum) for 1 day and subsequently exposed to IFN $\gamma$ . The cells were harvested, and RNA was isolated at the indicated times. In A, SM  $\alpha$ -actin mRNA abundance was measured by RPA as under “Experimental Procedures” ( $n = 3$ ;  $p < 0.05$  for IFN $\gamma$  versus control (–)). In B, following exposure to IFN $\gamma$  for 48 h, the cells were harvested and subjected to immunoblotting to detect SM  $\alpha$ -actin ( $\beta$ -actin was used as a loading control) ( $n = 3$ ;  $p < 0.05$  for IFN $\gamma$  versus control (–)). C, luciferase reporter constructs harboring different truncated SM  $\alpha$ -actin gene promoter (*Smpro*) fragments were transfected into stellate cells, and promoter activity was assayed ( $n = 3$ ;  $p < 0.01$  for IFN $\gamma$  versus control). D, SM  $\alpha$ -actin gene promoter CARG B and A boxes were mutated individually or combination. The resultant luciferase reporter constructs were transfected into stellate cells, and promoter activity was assayed ( $n = 3$ ;  $p < 0.01$  for IFN $\gamma$  versus control). *GAPDH*, glyceraldehyde-3-phosphate dehydrogenase; *IB*, immunoblot; *RLU*, relative light units.

antibodies against SRF, pSTAT1, and normal mouse and rabbit IgG were obtained from Santa Cruz; anti-acetylated H3 (H3Ac) and anti-P300 antibodies were from Upstate. Unless stated otherwise, the results have been presented as percentages relative to normalized sample input (the average raw volume of input samples was arbitrarily set to 1). The data from at least three individual experiments are presented graphically.

**Statistics**—All of the experiments were repeated at least three times, unless otherwise stated. A Student’s *t* test was used for comparison in experiments examining the effect of IFN $\gamma$  (*i.e.* +IFN $\gamma$  versus –IFN $\gamma$ ). The level of significance was considered to be  $p < 0.05$ .

**RESULTS**

**IFN $\gamma$ -mediated Inhibition of Smooth Muscle  $\alpha$ -Actin Expression Is Dependent on CARG Boxes**—We initially examined the effect of IFN $\gamma$  on smooth muscle  $\alpha$ -actin mRNA expression in activated stellate cells. As shown in Fig. 1A, the expression of smooth muscle  $\alpha$ -actin mRNA was significantly suppressed between 12 and 24 h after IFN $\gamma$  exposure. Concomitant with the effect of IFN $\gamma$  on smooth muscle  $\alpha$ -actin mRNA, smooth muscle  $\alpha$ -actin protein levels were also reduced (Fig. 1B). To explore the molecular mechanism by which IFN $\gamma$  exerts its inhibitory effect on smooth muscle  $\alpha$ -actin expression, we examined smooth muscle  $\alpha$ -actin transcriptional regulation.

Constructs harboring a series of rat smooth muscle  $\alpha$ -actin promoter fragments were generated and used to examine promoter activity. In Fig. 1C, it is shown that the Smpro-125 construct, which contains CARG-B and A boxes, generated a prominent response to IFN $\gamma$ : a 5-fold reduction of promoter activity compared with control. However, deletion of the CARG-B box (Smpro-109) resulted in marked reduction of promoter activity, which was almost complete after IFN $\gamma$  exposure. Because CARG boxes are known to be DNA-binding sites for SRF, these data suggest that the IFN $\gamma$ -mediated inhibitory effect on smooth muscle  $\alpha$ -actin gene promoter activity is linked to SRF.

To further examine the relationship between CARG boxes and the IFN $\gamma$ -mediated inhibitory effect on smooth muscle  $\alpha$ -actin promoter activity, we generated mutations in CARG-B and CARG-A boxes. Promoter activity for the wild type construct was reduced by 5-fold following IFN $\gamma$  treatment (Fig. 1D). In contrast, mutation of CARG-A or CARG-B boxes or both led to reduced promoter activity and a loss

of IFN $\gamma$  responsiveness. These data indicate that smooth muscle  $\alpha$ -actin promoter CARG-A and CARG-B boxes are critical in mediating the inhibitory effect of IFN $\gamma$  on smooth muscle  $\alpha$ -actin expression and that SRF is an important intermediate partner.

**IFN $\gamma$  Reduces SRF Expression and Binding to the Smooth Muscle  $\alpha$ -Actin Promoter**—Given previous data indicating that SRF is an essential transcription factor for multiple muscle-specific genes, we postulated that it might be a target of IFN $\gamma$ . To explore this possibility, we examined known IFN $\gamma$  signaling pathways in stellate cells. As predicted, IFN $\gamma$  exposure led to increases in STAT1 phosphorylation (pSTAT1) in both whole cell lysates and nuclear extracts (supplemental Fig. S1A). Next, we found that IFN $\gamma$  led to a significant reduction in SRF expression in stellate cells (Fig. 2A). Serum stimulation increased SRF expression and failed to elevate SRF in the presence of IFN $\gamma$  (Fig. 2B). These data indicate that SRF is a target of IFN $\gamma$  in stellate cells. Next, we examined whether the IFN $\gamma$ -mediated inhibition of SRF expression affected smooth muscle  $\alpha$ -actin promoter activity. Serum stimulation increased promoter activity compared with 0.1% serum-containing medium (Fig. 2C). However, IFN $\gamma$  abrogated this effect. These data suggest that the IFN $\gamma$ -induced inhibitory effect on smooth muscle  $\alpha$ -actin promoter activity occurs, at least in part, via reduction of SRF in stellate cells.



## IFN $\gamma$ Inhibits Smooth Muscle $\alpha$ -Actin via SRF

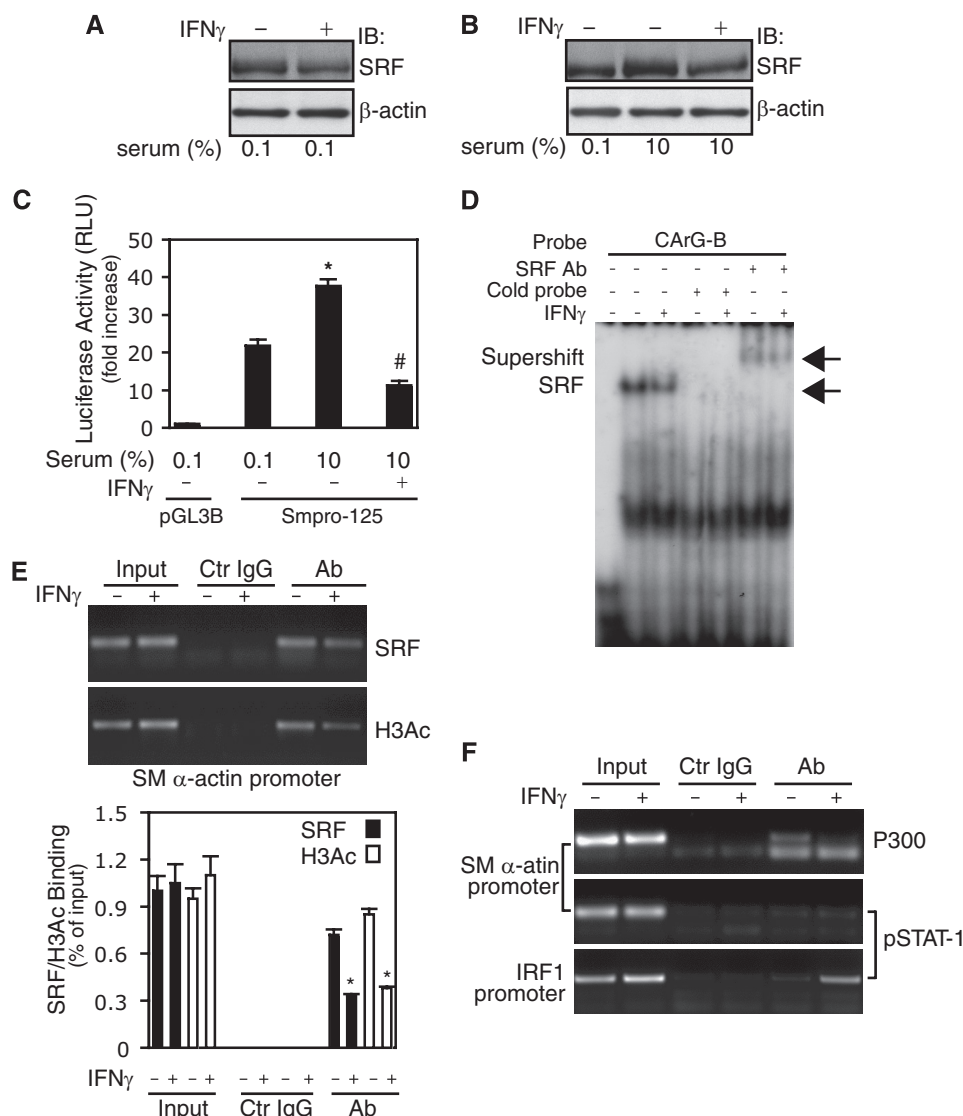


**FIGURE 2. IFN $\gamma$ -STAT1 pathway reduces SRF expression and binding to CArG boxes in smooth muscle  $\alpha$ -actin promoter.** *A*, stellate cells were starved (0.1% serum) for 1 day and incubated with IFN $\gamma$  for 2 days. Cell lysates were subjected to immunoblotting with anti-SRF antibody. *B*, stellate cells were starved (0.1% serum) for 1 day, then replaced with 10% serum-containing 199OR medium with or without IFN $\gamma$  for 2 days. Cell lysates were subjected to immunoblotting with anti-SRF antibody. *C*, following transduction with the Smpro-125 luciferase reporter construct, stellate cells were incubated in 0.1% serum-containing medium for 2 days, and then the medium was changed to 10% serum-containing medium with or without IFN $\gamma$  for a further 24 h. Cell lysates were assayed for luciferase activity ( $n = 3$ ; \*,  $p < 0.01$  for 0.1% versus 10% serum-containing medium; #,  $p < 0.01$  for IFN $\gamma$  versus control). *D*, after incubation with 0.1% serum-containing medium for 1 day, stellate cells were exposed to IFN $\gamma$  for 2 days, and nuclear extracts were prepared for EMSA with a probe containing the CArG-B box of SM  $\alpha$ -actin gene promoter. The left-most lane contains buffer plus labeled probe only (*i.e.* without nuclear extract). The arrows denote the SRF and probe complex or a supershift complex with SRF antibody. *E* and *F*, stellate cells were starved (0.1% serum) for 1 day and exposed to IFN $\gamma$  for 16 h; cells were subjected to ChIP assay as under "Experimental Procedures". In *E*, the data are depicted graphically below ( $n = 3$ ; \*,  $p < 0.01$  for IFN $\gamma$  versus control). *IB*, immunoblot; *Ab*, antibody; *Ctrl*, control.

Because smooth muscle  $\alpha$ -actin promoter activity is SRF-dependent (Fig. 1D), we examined whether IFN $\gamma$  might inhibit SRF binding activity. In these experiments, a probe containing the CArG-B box of smooth muscle  $\alpha$ -actin promoter was utilized. Nuclear extracts from stellate cells exposed to IFN $\gamma$  had a weaker shifted band compared with control (Fig. 2D). The addition of anti-SRF antibody and cold probe demonstrated that the SRF binding was specific. These data suggest that IFN $\gamma$  reduces nuclear SRF binding in stellate cells. Further, we examined whether IFN $\gamma$  decreased SRF binding to smooth muscle  $\alpha$ -actin

promoter CArG boxes *in vivo*. Following exposure of stellate cells to IFN $\gamma$  for 16 h, SRF binding to smooth muscle  $\alpha$ -actin promoter CArG boxes was dramatically reduced compared with control (Fig. 2E). Interestingly, decreased binding of SRF to smooth muscle  $\alpha$ -actin promoter CArG boxes was accompanied by reduced binding of H3Ac, which itself is associated with gene transcriptional activation (21). We also found that IFN $\gamma$  reduced both SRF and H3Ac binding to smooth muscle  $\alpha$ -actin promoter CArG boxes even under serum stimulation (supplemental Fig. S1B). Because p300, a transcriptional coactivator, plays a critical role in gene regulation through histone acetylation and interaction with a variety of transcriptional factors such as STAT1 (22), we examined whether p300 and STAT1 might form DNA-protein complexes in the smooth muscle  $\alpha$ -actin promoter *in vivo*. As shown in Fig. 2F (top panel), p300 was found in control, but after exposure to IFN $\gamma$ , p300 in the smooth muscle  $\alpha$ -actin promoter essentially disappeared, consistent with the reduced amount of H3Ac in the smooth muscle  $\alpha$ -actin promoter after IFN $\gamma$  (Fig. 2E). In contrast, we could not identify pSTAT1 in the smooth muscle  $\alpha$ -actin promoter (Fig. 2F, middle panel; as a control, pSTAT1 was readily identified in the interferon regulatory factor 1 gene promoter, Fig. 2F, bottom panel). Taken together, these data demonstrate that both SRF expression and binding activity to smooth muscle  $\alpha$ -actin promoter CArG boxes were significantly reduced by IFN $\gamma$ . IFN $\gamma$  also induced negative epigenetic regulation of smooth muscle  $\alpha$ -actin through reducing

smooth muscle  $\alpha$ -actin promoter histone 3 acetylation.

**IFN $\gamma$  Inhibits SRF Expression through Its Own Transcriptional Regulation**—To further explore the molecular mechanism by which IFN $\gamma$  down-regulates SRF, we cloned a 798-bp fragment in the proximal SRF gene promoter region from stellate cells and tested the effects of IFN $\gamma$  on SRF transcription. SRF promoter activity was dramatically suppressed by IFN $\gamma$  (Fig. 3A). Next, we asked whether IFN $\gamma$ -mediated suppression of SRF promoter activity could be associated with the serum response elements of the SRF gene promoter. As shown in

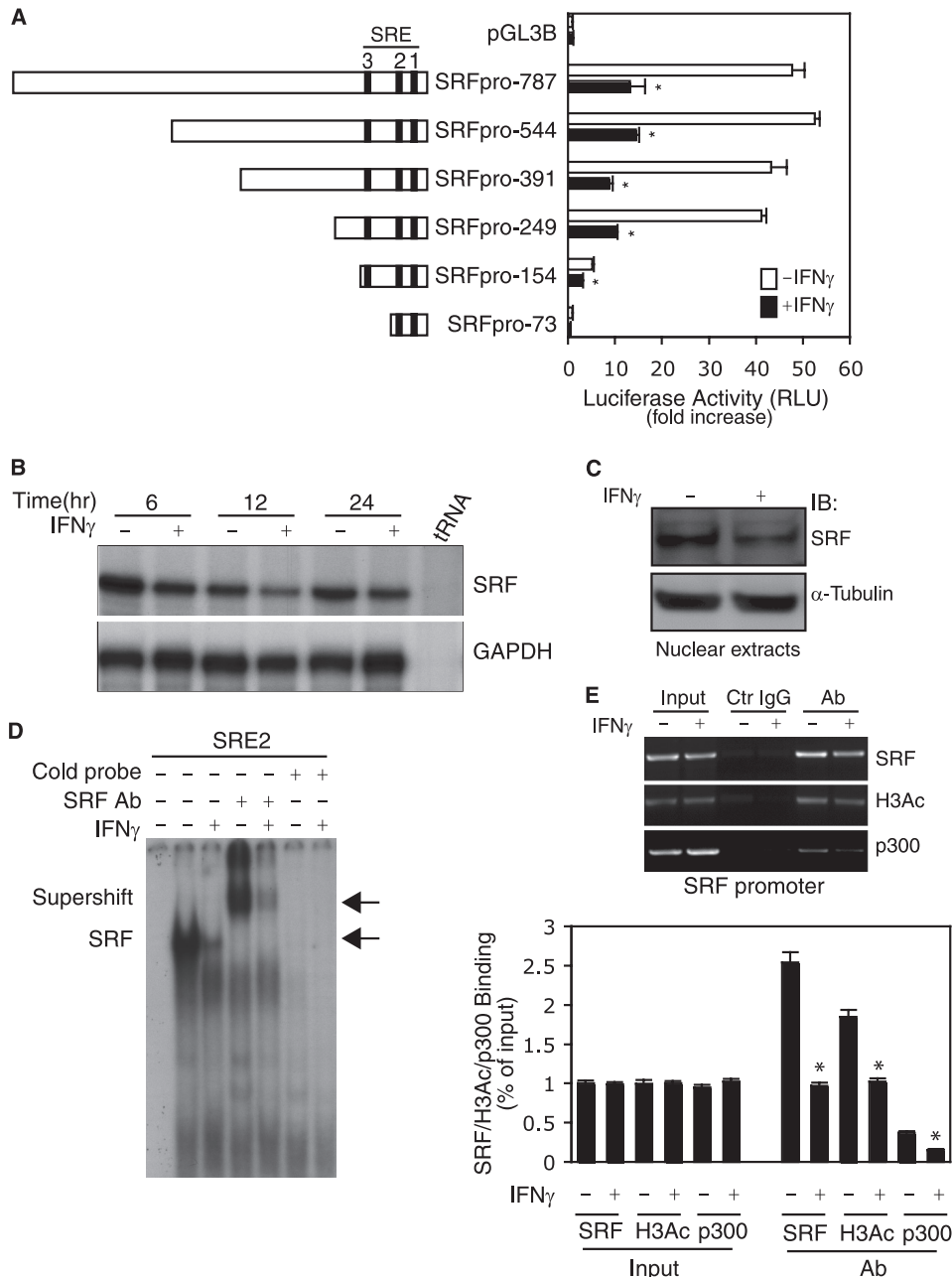


**FIGURE 3. IFN $\gamma$  inhibits SRF promoter activity and reduces SRF binding to CaRG boxes in the SRF promoter.** *A*, stellate cells were transfected with truncated SRF reporter constructs as indicated and then incubated in 0.1% serum-containing 199OR medium with or without IFN $\gamma$  for 2 days. The cell lysates were assayed to detect SRF promoter activity ( $n = 3$ ;  $*$ ,  $p < 0.01$  for IFN $\gamma$  versus control). *B*, stellate cells were starved (0.1% serum) for 1 day and exposed to IFN $\gamma$  at indicated time points. Total RNA was extracted, and SRF mRNA levels were measured by RPA. *C* and *D*, stellate cells were starved in 0.1% serum-containing 199OR medium for 1 day and exposed to IFN $\gamma$  for 2 days. SRF was detected in nuclear extracts by immunoblotting (*C*) and EMSA (*D*). The *left-most lane* contains buffer plus labeled probe only (*i.e.* without nuclear extract). The *arrows* denote SRF and probe complex and supershift complex with SRF antibody (*D*). *E*, stellate cells were starved (0.1% serum) for 1 day and exposed to IFN $\gamma$  for 16 h. SRF binding activity to its own promoter was examined by ChIP assay. The data are depicted graphically below ( $n = 3$ ;  $*$ ,  $p < 0.01$  for IFN $\gamma$  versus control). GAPDH, glyceraldehyde-3-phosphate dehydrogenase; IB, immunoblot; Ctr, control; Ab, antibody.

supplemental Fig. S2, all of the serum response elements appeared to be required for maintenance of full SRF promoter activity. Mutation of serum response elements 1 and 2 in the SRF promoter substantially abrogated the inhibitory effect of IFN $\gamma$  on SRF promoter activity. These data led us to further hypothesize that IFN $\gamma$  could reduce SRF mRNA levels. As

expected, SRF mRNA expression was reduced at all time points after IFN $\gamma$  exposure compared with control (Fig. 3*B*). However, the most prominent SRF mRNA reduction occurred at the 12-h time point, which correlated with the most significant reduction in smooth muscle  $\alpha$ -actin mRNA (Fig. 1*A*). Given the finding that IFN $\gamma$  down-regulated SRF mRNA expression, we further hypothesized that SRF levels in stellate cell nuclei would likewise be reduced, in turn leading to reduced SRF binding to its own gene promoter. To test this postulate, we examined SRF levels in stellate cell nuclear extracts as well as SRF binding activity to SRF promoter CaRG boxes *in vitro* and *in vivo*. IFN $\gamma$  decreased SRF in stellate cell nuclei (Fig. 3*C*). SRF binding to its CaRG boxes was reduced following IFN $\gamma$  exposure (Fig. 3, *D* and *E*). Additionally, H3Ac and p300 were reduced in the SRF promoter after IFN $\gamma$  exposure. These findings were similar to those found with the smooth muscle  $\alpha$ -actin promoter (Fig. 2).

We next examined whether two potential  $\gamma$ -activated sites (GAS) (23) in the SRF promoter might modulate SRF expression. As shown in supplemental Fig. 3*A*, pSTAT1 did not appear to form a DNA-protein complex with either of the two putative SRF GAS elements. Although cross-linked DNA-pSTAT1 complexes could be readily identified in the lysates from cells exposed to IFN $\gamma$  (supplemental Fig. 3*B*), specific DNA fragments harboring GAS elements from the SRF gene promoter were undetectable whether exposed to IFN $\gamma$  or not (supplemental Fig. S3*C*, upper panel). In contrast, a DNA fragment containing the interferon regulatory factor 1 GAS element was identified (supplemental Fig. S3*C*, lower panel). These data suggest that IFN $\gamma$ -mediated down-regulation of SRF occurs via pathways other than

by direct targeting of SRF gene transcription.

**IFN $\gamma$ -mediated Down-regulation of Smooth Muscle  $\alpha$ -Actin and SRF Is STAT1-dependent**—Because IFN $\gamma$  exerts its effects through both STAT1-dependent and -independent pathways (24), we studied stellate cells from STAT1<sup>+/+</sup> (wild type) and STAT1<sup>-/-</sup> (knock-out) mice. Stellate cells from

## IFN $\gamma$ Inhibits Smooth Muscle $\alpha$ -Actin via SRF

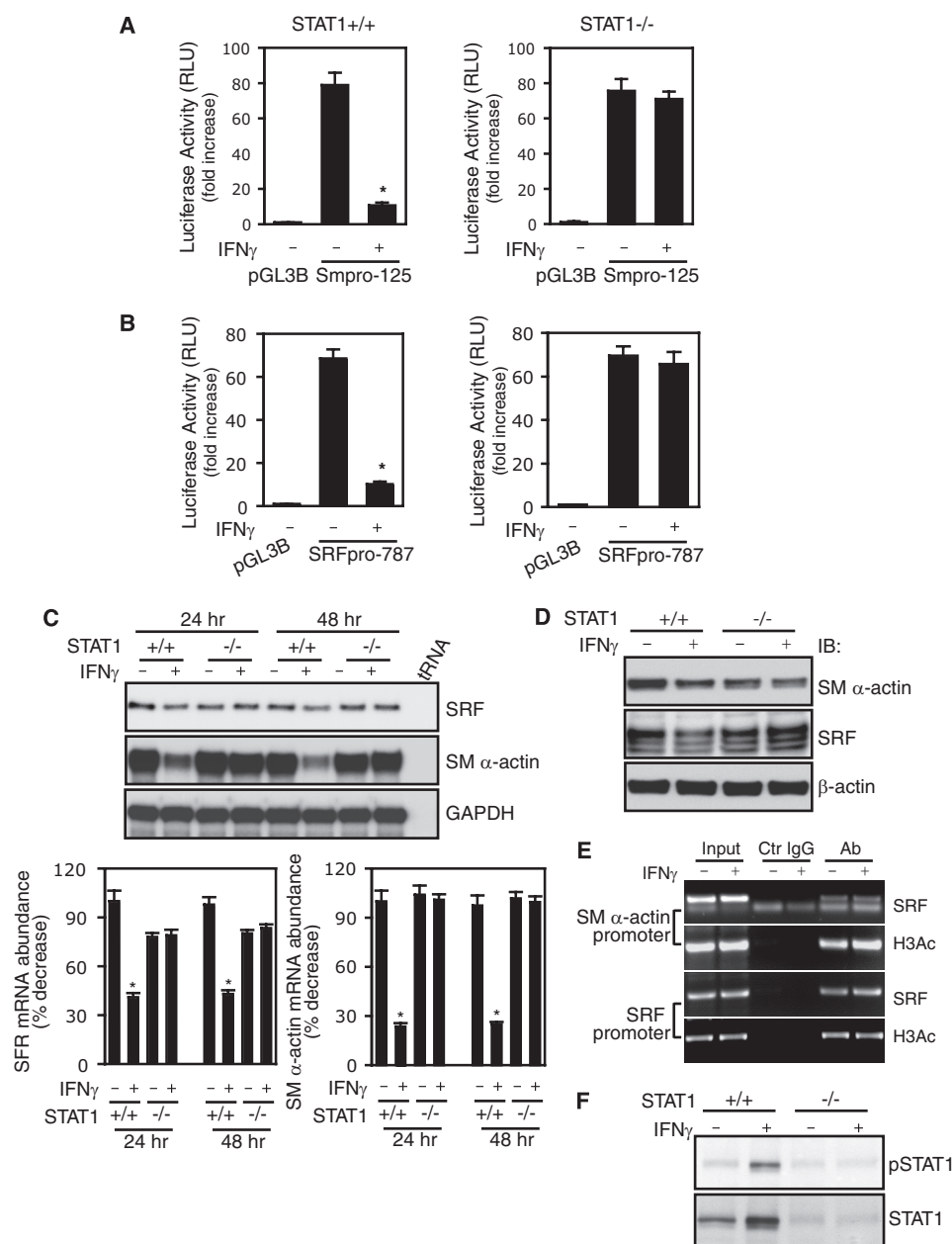


**FIGURE 4. STAT1 is required for IFN $\gamma$ -induced down-regulation of smooth muscle  $\alpha$ -actin and SRF.** A and B, stellate cells from STAT1 wild type (+/+) and STAT1 knock-out (-/-) mice were transfected with SM  $\alpha$ -actin (A) or SRF (B) reporter constructs as indicated. The cells were incubated in 0.1% serum-containing medium with or without IFN $\gamma$  for 2 days before harvest ( $n = 3$ ;  $p < 0.01$  for IFN $\gamma$  versus control). C, stellate cells from wild type and STAT1 knock-out mice were serum-starved for 1 day and then exposed to IFN $\gamma$  for 24 or 48 h. SM  $\alpha$ -actin and SRF mRNA levels were measured by RPA. The data were quantitated and are depicted graphically below ( $n = 3$ ;  $p < 0.01$  for IFN $\gamma$  versus control). D, stellate cells were starved (0.1% serum) for 1 day and incubated with or without IFN $\gamma$  for 2 days. The cell lysates were immunoblotted with specific antibodies as indicated. E, stellate cells from STAT1<sup>-/-</sup> mice were serum-starved for 1 day and exposed to IFN $\gamma$  for 16 h. ChIP assay was performed as in Fig. 2E. F, genotypes of wild type and STAT1 knock-out stellate cells were further verified by immunoblotting. RLU, relative light units; GAPDH, glyceraldehyde-3-phosphate dehydrogenase; IB, immunoblot; Ab, antibody; Ctr, control.

STAT1<sup>+/+</sup> mice (Fig. 4A, left panel) and STAT1<sup>-/-</sup> mice (Fig. 4A, right panel) exhibited remarkably different promoter activity responses to IFN $\gamma$ . Smooth muscle  $\alpha$ -actin promoter activity was reduced by IFN $\gamma$  in stellate cells from STAT1<sup>+/+</sup> mice but not in those from STAT1<sup>-/-</sup> mice. Similar results were obtained in experiments with SRF promoter constructs (Fig. 4B), in which the inhibitory effect of IFN $\gamma$  on SRF promoter activity was abrogated in STAT1-deficient

stellate cells (Fig. 4B, right panel). The results suggest that IFN $\gamma$ -induced inhibitory effects on smooth muscle  $\alpha$ -actin and SRF promoter activity are both STAT1-dependent.

Given the evidence that STAT1 is required for the negative effects of IFN $\gamma$  on both smooth muscle  $\alpha$ -actin and SRF promoter activity, we reasoned that IFN $\gamma$ -mediated down-regulation of smooth muscle  $\alpha$ -actin and SRF gene expression would be abrogated in STAT1-deficient stellate cells. As predicted, SRF and smooth muscle  $\alpha$ -actin mRNA expression were reduced in stellate cells from STAT1<sup>+/+</sup> mice after IFN $\gamma$  exposure (Fig. 4C). However, smooth muscle  $\alpha$ -actin and SRF mRNA levels were not reduced by IFN $\gamma$  in STAT1-deficient stellate cells. Immunoblot analyses paralleled mRNA findings (Fig. 4D). We further examined whether STAT1 is required for IFN $\gamma$ -mediated inhibition of SRF binding activity and histone 3 acetylation in both smooth muscle  $\alpha$ -actin and SRF promoters. IFN $\gamma$  failed to reduce SRF and H3Ac binding activity in both promoters in STAT1-deficient stellate cells (Fig. 4E). Further, we examined pSTAT1 levels in stellate cells from STAT1<sup>+/+</sup> and STAT1<sup>-/-</sup> mice (Fig. 4F). pSTAT1 was readily detected in STAT1<sup>+/+</sup> stellate cells following IFN $\gamma$  but was undetectable in stellate cells from STAT1<sup>-/-</sup> mice.

**IFN $\gamma$  Induces SRF mRNA Degradation in a STAT1-dependent Manner**—It is well known that mRNA stability plays an important role in determining levels of gene expression (25). We further examined whether IFN $\gamma$  might contribute to SRF mRNA degradation in stellate cells. We first cloned the rat SRF mRNA 3'-UTR region and examined mRNA decay

with a luciferase reporter; IFN $\gamma$  significantly reduced luciferase activity (Fig. 5A), suggesting that IFN $\gamma$  likely targets SRF mRNA stability. Next, we examined whether IFN $\gamma$  might contribute to SRF mRNA degradation in stellate cells. IFN $\gamma$  led to a persistent decrease in SRF mRNA levels, whereas SRF mRNA levels in control samples remained stable (Fig. 5B). We further examined whether IFN $\gamma$  enhances SRF mRNA decay under actinomycin D treatment. The cells



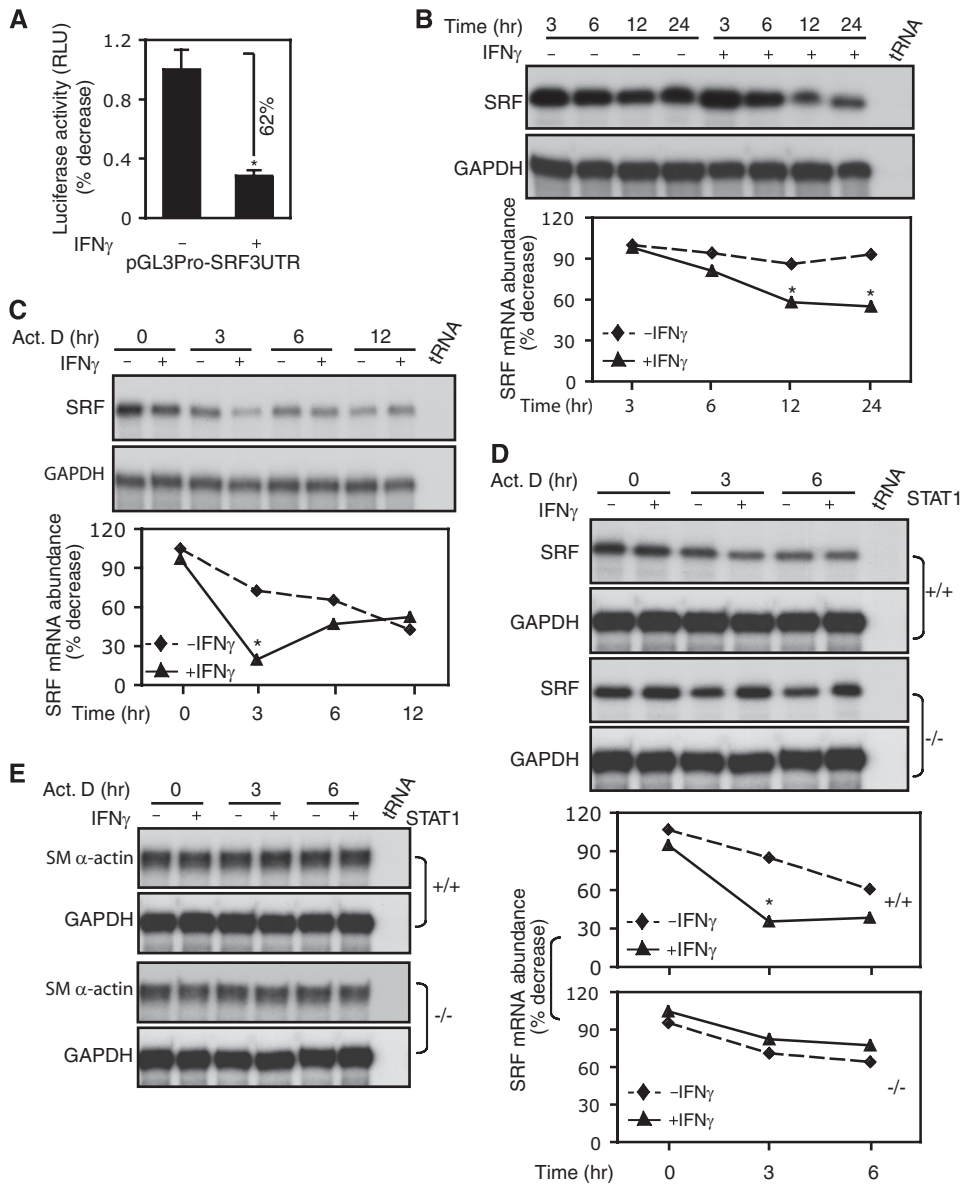


**FIGURE 5. IFN $\gamma$  induces SRF mRNA degradation but has no effect on smooth muscle  $\alpha$ -actin mRNA stability.** A, following transfection with a SRF mRNA 3'-UTR-luciferase report construct, stellate cells were exposed to IFN $\gamma$  for 2 days, and luciferase activity was measured in cell lysates ( $n = 3$ ;  $*$ ,  $p < 0.05$  for IFN $\gamma$  versus control). B, following serum starvation (0.1%) for 1 day, stellate cells were exposed to IFN $\gamma$  for various periods of time, and total RNA was subsequently extracted and subjected to RPA. The data were quantitated and are depicted graphically below ( $n = 3$ ;  $*$ ,  $p < 0.01$  for IFN $\gamma$  versus control). C, stellate cells were starved (0.1% serum) for 1 day. The cells were exposed to IFN $\gamma$  for 2 h and then incubated with actinomycin D (10  $\mu$ g/ml). Total RNA was subsequently extracted and subjected to RPA. The data were quantitated and are depicted graphically below ( $n = 3$ ;  $*$ ,  $p < 0.01$  for IFN $\gamma$  versus control). D and E, stellate cells from wild type (+/+) and STAT1 knock-out (-/-) mice were subjected to mRNA decay assay as in C. The data were quantitated and are depicted graphically ( $n = 3$ ;  $*$ ,  $p < 0.01$  for IFN $\gamma$  versus control in C). GAPDH, glyceraldehyde-3-phosphate dehydrogenase; Act. D, actinomycin D.

were exposed to IFN $\gamma$  for 2 h to activate the IFN $\gamma$  signal pathway (supplemental Fig. S1A) and then incubated with actinomycin D. SRF mRNA was decreased at the 3-h time point compared with controls (Fig. 5C). These results suggest that IFN $\gamma$  is able to activate SRF mRNA degradation machinery in stellate cells.

Given that IFN $\gamma$  down-regulated SRF mRNA expression via a STAT1-dependent pathway, we further hypothesized that deletion of STAT1 would abrogate IFN $\gamma$ -mediated SRF mRNA decay in stellate cells. As predicated, IFN $\gamma$  led to

degradation of SRF mRNA in stellate cells from STAT1<sup>+/+</sup> mice, similar to rat stellate cells (Fig. 5D). Notably, IFN $\gamma$  failed to induce SRF mRNA degradation in STAT1-deficient stellate cells (Fig. 5D). These data suggest that IFN $\gamma$  targets the SRF gene via post-transcriptional STAT1-mediated SRF mRNA degradation.

Furthermore, we explored whether IFN $\gamma$  might induce smooth muscle  $\alpha$ -actin mRNA degradation, which would contribute to the reduction in smooth muscle  $\alpha$ -actin expression. Compared with SRE, IFN $\gamma$  had little effect on smooth muscle  $\alpha$ -actin mRNA stability in stellate cells (Fig. 5E), suggesting that IFN $\gamma$  reduces smooth muscle  $\alpha$ -actin expression not directly but by regulation of SRF.

*The 2-5A Synthetase-RNase L System Mediates IFN $\gamma$ -induced SRF mRNA Decay*—To explore the pathways leading to SRF mRNA decay, we first examined the 2-5A system, an RNA degradation pathway that can be induced by IFNs (26). IFN $\gamma$  increased 2-5A synthetase mRNA levels ~5-fold compared with control (Fig. 6A). Because 2-5A synthetase generates 2-5A and activates RNase L, we hypothesized that RNase L might also respond to IFN $\gamma$  stimulation. As shown in Fig. 6B, RNase L mRNA levels were robustly stimulated by IFN $\gamma$  compared with control. Next, we examined whether RNase L targets SRF mRNA by using RNase L<sup>-/-</sup> MEFs (27). IFN $\gamma$  reduced SRF mRNA levels in RNase L<sup>+/+</sup> MEFs but failed to reduce SRF mRNA levels in RNase L-deficient MEFs (Fig. 6C). The results suggested that RNase L plays a critical role in IFN $\gamma$ -mediated SRF mRNA degradation. We next examined SRF protein levels in RNase L<sup>-/-</sup> and RNase L<sup>+/+</sup> MEFs following IFN $\gamma$  exposure. IFN $\gamma$  led to a reduction in SRF expression in wild type but not knock-out RNase L MEFs (Fig. 6D, top panel), consistent with the SRF mRNA levels depicted in Fig. 6C.

Because RNase L has been shown to regulate skeletal muscle cell differentiation (28), we postulated that it may also regulate smooth muscle programs. Interestingly, smooth muscle  $\alpha$ -actin expression was detected in RNase L<sup>-/-</sup> MEFs but not in

## IFN $\gamma$ Inhibits Smooth Muscle $\alpha$ -Actin via SRF

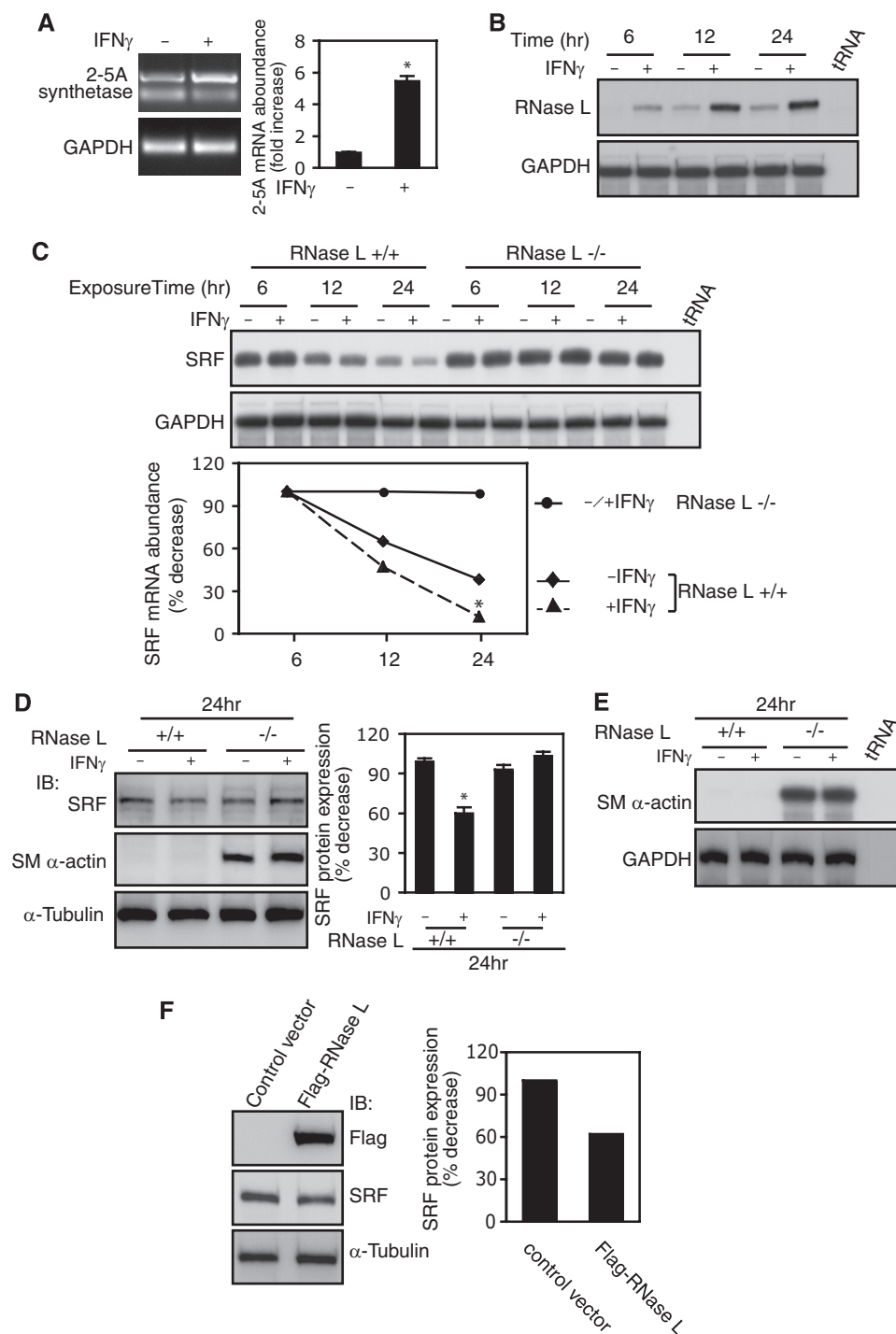


**FIGURE 6. SRF is a novel target gene of IFN $\gamma$ -induced 2-5A-RNase L system.** *A*, stellate cells were serum-starved (0.1%) for 1 day and exposed to IFN $\gamma$  for 24 h. 2-5A synthetase 1A mRNA expression was determined by RT-PCR ( $n = 3$ ; \*,  $p < 0.05$  for IFN $\gamma$  versus control). *B* and *C*, RNase L $^{+/+}$  (*B*) and RNase L $^{-/-}$  (*C*) MEFs were serum-starved (0.2%) for 1 day and exposed to IFN $\gamma$  at the indicated time points. RNase L (*B*) and SRF (*C*) mRNA expression were measured by RPA. In *C*, the data were quantitated and are depicted graphically ( $n = 3$ ; \*,  $p < 0.05$  for IFN $\gamma$  versus control in RNase L $^{+/+}$  MEFs). *D* and *E*, RNase L $^{+/+}$  and RNase L $^{-/-}$  MEFs were serum-starved (0.2%) for 1 day and exposed to IFN $\gamma$  for 24 h. In *D*, cell lysates were subjected to immunoblotting with specific antibodies as indicated. The data were quantitated and are depicted graphically ( $n = 3$ ; \*,  $p < 0.05$  for IFN $\gamma$  versus control in RNase L $^{+/+}$  MEFs). In *E*, SM  $\alpha$ -actin mRNA expression was measured by RPA. *F*, HEK293 cells were transfected with a mouse FLAG-RNase L expression construct or an empty vector overnight and incubated in 0.2% serum-containing medium for 24 h, and nuclear extracts were subjected to immunoblotting with specific antibodies as indicated. SRF bands were quantitated and shown in the graph on the right. GAPDH, glyceraldehyde-3-phosphate dehydrogenase; IB, immunoblot.

RNase L $^{+/+}$  MEFs at both protein (Fig. 6*D*, middle panel) and mRNA levels (Fig. 6*E*). Notably, IFN $\gamma$ -induced inhibition of smooth muscle  $\alpha$ -actin expression was abrogated in RNase L null MEFs (Fig. 6, *D* and *E*), which paralleled SRF levels in these cells (Fig. 6, *C* and *D*, top panel). Furthermore, overexpression of RNase L led to decreased SRF levels in HKE293 cells compared with the control (Fig. 6*F*). Taken together, these data indicated that SRF is a new molecular target in the IFN $\gamma$ -induced 2-5A-RNase L pathway, which plays a critical role in IFN $\gamma$ -induced SRF mRNA degradation.

*IFN $\gamma$ -induced Inhibition of SMMHC mRNA Expression Links to Decreased SRF Binding in CARG Box of SMMHC Promoter*—In addition to smooth muscle  $\alpha$ -actin, SMMHC is another smooth muscle cell and myofibroblast marker, whose expression, at least in smooth muscle cells, is also tightly controlled by SRF (5). Therefore, we examined whether IFN $\gamma$ -induced targeting of SRF might affect SMMHC mRNA expression. SMMHC mRNA expression was reduced at all time points following IFN $\gamma$  exposure (Fig. 7*A*). Promoter analysis indicated that IFN $\gamma$ -induced reduction of luciferase activity was closely linked to CARG boxes in the SMMHC promoter (Fig. 7*B*). Next, we examined SRF binding activity to the SMMHC promoter CARG box. As predicted, IFN $\gamma$  caused a reduction in SRF binding to the SMMHC promoter CARG box compared with control (Fig. 7*C*). These data provide further evidence for the prominent effect of IFN $\gamma$  on SRF (and thus a repertoire of smooth muscle-specific gene expression).

## DISCUSSION

In this study, we have identified a novel target of IFN $\gamma$ , namely SRF. We have also discovered a novel IFN $\gamma$ -induced SRF mRNA decay-promoting pathway that involves the 2-5A-RNase L system. Together, this pathway makes up a novel signaling network from IFN $\gamma$  to SRF and smooth muscle protein



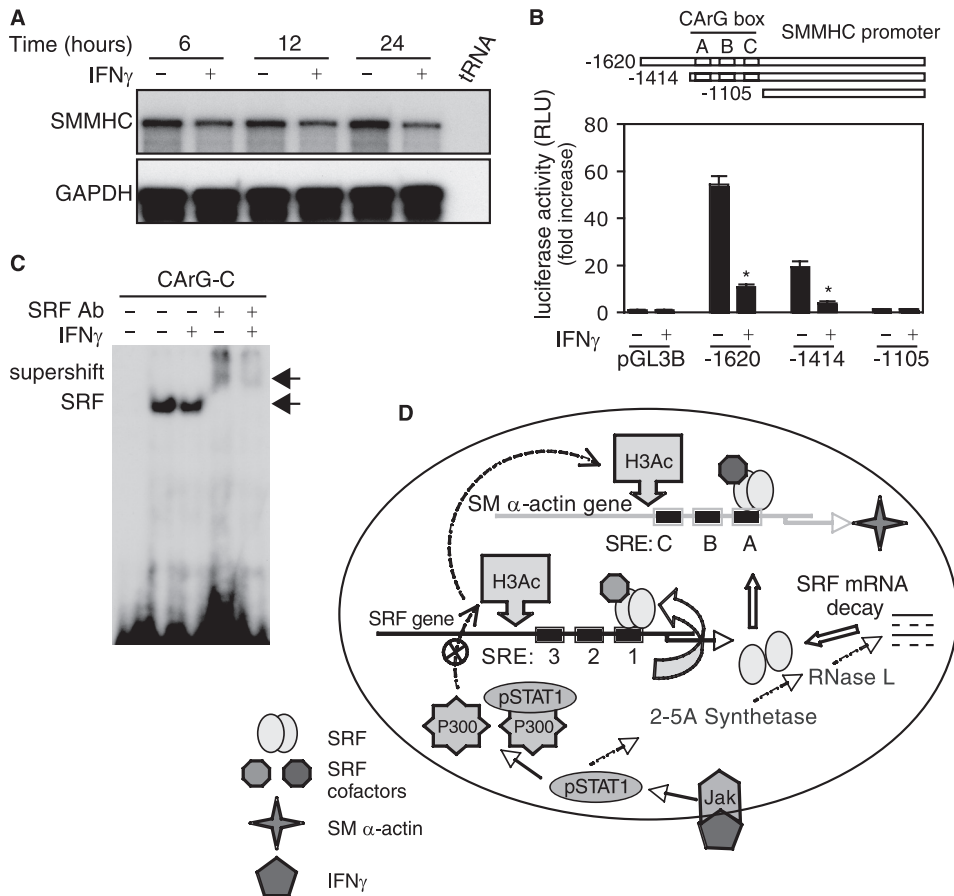


**FIGURE 7. IFN $\gamma$  inhibits SMMHC mRNA expression and SRF binding to SMMHC promoter CARG boxes.** A, stellate cells were serum-starved (0.1% serum) for 1 day and exposed to IFN $\gamma$  at the indicated time points. Total RNA was isolated, and SMMHC mRNA expression was measured by RPA. B, a luciferase reporter plasmid harboring different truncated SMMHC promoter fragments was created as in the top panel. Following transfection, stellate cells were incubated in 0.1% serum-containing medium with or without IFN $\gamma$  for 2 days. Cell lysates were assayed for luciferase activity ( $n = 3$ ; \*,  $p < 0.05$  for IFN $\gamma$  versus control). C, stellate cells were serum-starved (0.1% serum) for 1 day and exposed to IFN $\gamma$  for 2 days. Nuclear extracts were subjected to EMSA. The arrows denote shifted bands and supershift with SRF antibody. The first lane on the left contains buffer plus labeled probe only (i.e. without nuclear extract). D, an overview of the IFN $\gamma$ -SRF signaling pathway is highlighted. GAPDH, glyceraldehyde-3-phosphate dehydrogenase; Ab, antibody; RLU, relative light units.

expression (Fig. 7D). In the context of IFN $\gamma$  biology, our work is consistent with previous studies emphasizing a number of IFN $\gamma$ -regulated genes. Further, elucidation of such targets is critical for understanding IFN $\gamma$ -mediated biological effects (1, 3, 29).

Abundant evidence links IFN $\gamma$  to fibrogenesis, and this cytokine has been proposed as a putative therapy for fibrosis (17, 30, 31). In the wounding milieu, IFN $\gamma$  exhibits prominent inhibitory effects on fibroblasts and myofibroblasts, including hepatic stellate cells, liver-specific myofibroblasts. Myofibroblasts are characterized by *de novo* expression of smooth muscle  $\alpha$ -actin and excessive production of extracellular matrix, particularly collagen type 1 (32). Although the mechanisms for IFN $\gamma$ -mediated inhibition of collagen type 1 expression have been well described (33), the molecular mechanism by which IFN $\gamma$  inhibits smooth muscle  $\alpha$ -actin expression appears to be different. Specifically, the effect of IFN $\gamma$  on myofibroblasts appears to be tightly linked to SRF regulation. Here, we have demonstrated that the binding activity of SRF to the smooth muscle  $\alpha$ -actin promoter (CARG boxes) is reduced by IFN $\gamma$  (Figs. 1 and 2). This occurs as a result of IFN $\gamma$  targeting SRF (Fig. 2). We speculate

that IFN $\gamma$ -mediated inhibition of SRF (Figs. 2 and 3) is likely to be a critical modulator of myofibroblast differentiation in wound healing, because SRF targets the promoters of multiple smooth muscle genes that are expressed in myofibroblasts. In support of this position is our finding that not only did IFN $\gamma$  inhibit smooth muscle  $\alpha$ -actin but also it potentially inhibited SMMHC promoter activity (Fig. 7B). Further, because SRF is also regulated in an apparent feedback loop (18), it is possible that reduction of SRF by IFN $\gamma$  likely has indirect effects on its own promoter activity (supplemental Fig. S2). Interestingly, reduced SRF binding in the smooth muscle  $\alpha$ -actin and SRF promoters was closely linked to decreased p300 and H3Ac binding (Figs. 2 and 3), which further led to decreased SRF and smooth muscle  $\alpha$ -actin expression through IFN $\gamma$ -induced negative epigenetic regulation.

Although IFN $\gamma$  is able to signal via STAT1-independent pathways, the IFN $\gamma$ -STAT1 pathway likely mediates the majority of IFN $\gamma$ -induced biological effects, which have been well demonstrated in STAT1 gene knock-out animal models (34). Our data are highly consistent with this position, as specifically demonstrated in Figs. 4 and 5. The finding that STAT1 deletion completely

abrogated IFN $\gamma$ -mediated SRF mRNA decay (Fig. 5) and previous work linking STAT1 to 2-5A synthetase/RNase L (26) led us to explore the possibility that the 2-5A synthetase/RNase L signal pathway could play a role in our system. We found that IFN $\gamma$  regulated SRF mRNA stability in a 2-5A synthetase/RNase L-dependent manner (Fig. 6). Thus, our data have also highlighted an additional novel target (i.e. SRF) of the 2-5A synthetase/RNase L system. A surprising finding in our study was that smooth muscle  $\alpha$ -actin expression was activated in RNase L-deficient MEFs (Fig. 6, D and E). This finding implicates the 2-5A synthetase/RNase L system in control of smooth muscle gene transcriptional activation through regulation of SRF and/or SRF cofactors. For example, it remains to be determined whether RNase L also targets the SRF cofactor, myocardin, whose expression was tightly linked to smooth muscle-specific gene expression including smooth muscle  $\alpha$ -actin and SMMHC (35).

RNase L is a latent endoribonuclease whose activity appears to be tightly regulated by 2-5A. Furthermore, 2-5A is generated by 2-5A synthetase, which is induced by IFNs (36). Importantly, the effects of 2-5A are transient, because 2-5A is unstable

## IFN $\gamma$ Inhibits Smooth Muscle $\alpha$ -Actin via SRF

due to the activities of phosphodiesterases and phosphatases (37). Such a sensitive regulatory cascade appears to be important for regulating protein synthesis via mRNA degradation in response to exogenous stimuli. In our study, IFN $\gamma$ -induced 2-5A synthetase and RNase L expression rapidly increased at  $\sim$ 12 h (Fig. 6, A and B); simultaneously, SRF/smooth muscle  $\alpha$ -actin mRNA levels reached their lowest point at  $\sim$ 12 h (3 h with actinomycin D) and then gradually rebounded (Figs. 1, 2, 3, and 5). The phenomenon of SRF mRNA rebound was highly reproducible and likely reflects a crucial effect of RNase L in regulation of SRF mRNA stability (Fig. 6) as well as the complex nature of the SRF mRNA regulatory machinery. Nonetheless, these data integrate IFN $\gamma$ -STAT1 signaling with the 2-5A/RNase L system, SRF, and SRF target genes and provide a framework for a complicated molecular regulatory network for IFN $\gamma$ -mediated inhibition of smooth muscle-specific gene expression (Fig. 7D).

Identification of SRF as a novel target of IFN $\gamma$  in myofibroblasts has implications not only for wound healing but also in vascular biology and perhaps even oncogenesis. It is well appreciated that SRF plays a central role in smooth muscle cell differentiation, which is characterized by expression of a unique repertoire of contractile proteins, such as smooth muscle  $\alpha$ -actin and SMMHC. Vascular diseases such as atherosclerosis are characterized by dysregulation of contractile protein expression in smooth muscle cells, and it is likely that SRF plays a role in regulation of these proteins (10). Further, SRF expression appears to be linked to cancer invasion/metastasis (38). Thus, although speculative, our data raise the possibility that the IFN $\gamma$ -SRF signaling pathway identified here could be important in oncogenesis. Finally, the complicated nature by which SRF is regulated in our system and in other studies implies a highly complex regulatory hierarchy and suggests that efforts to manipulate SRF biologically will be challenging.

*Acknowledgments*—We thank Yingyu Ren for expert assistance with rat and mouse stellate cell isolation and culture and Tianxia Li for assistance with RNase protection assays and immunoblots. We thank R. H. Silverman for RNase L<sup>-/-</sup> and RNase L<sup>+/+</sup> MEF cell lines and S. L. White for the rat SMMHC gene promoter plasmid.

## REFERENCES

- Boehm, U., Klamp, T., Groot, M., and Howard, J. C. (1997) *Annu. Rev. Immunol.* **15**, 749–795
- Dunn, G. P., Koebel, C. M., and Schreiber, R. D. (2006) *Nat. Rev. Immunol.* **6**, 836–848
- Der, S. D., Zhou, A., Williams, B. R., and Silverman, R. H. (1998) *Proc. Natl. Acad. Sci. U.S.A.* **95**, 15623–15628
- Schroder, K., Hertzog, P. J., Ravasi, T., and Hume, D. A. (2004) *J. Leukocyte Biol.* **75**, 163–189
- Owens, G. K., Kumar, M. S., and Wamhoff, B. R. (2004) *Physiol. Rev.* **84**, 767–801
- Hinz, B., Phan, S. H., Thannickal, V. J., Galli, A., Bochaton-Piallat, M. L., and Gabbiani, G. (2007) *Am. J. Pathol.* **170**, 1807–1816
- Thiery, J. P., Acloque, H., Huang, R. Y., and Nieto, M. A. (2009) *Cell* **139**, 871–890
- Hansson, G. K., Hellstrand, M., Rymo, L., Rubbia, L., and Gabbiani, G. (1989) *J. Exp. Med.* **170**, 1595–1608
- Rockey, D. C., Maher, J. J., Jarnagin, W. R., Gabbiani, G., and Friedman, S. L. (1992) *Hepatology* **16**, 776–784
- Miano, J. M., Long, X., and Fujiwara, K. (2007) *Am. J. Physiol. Cell. Physiol.* **292**, C70–C81
- Yoshida, T., Hoofnagle, M. H., and Owens, G. K. (2004) *Circ. Res.* **94**, 1075–1082
- Wang, J., Zohar, R., and McCulloch, C. A. (2006) *Exp. Cell. Res.* **312**, 205–214
- Herrmann, J., Haas, U., Gressner, A. M., and Weiskirchen, R. (2007) *Biochim. Biophys. Acta* **1772**, 1250–1257
- Sandbo, N., Kregel, S., Taurin, S., Bhorade, S., and Dulin, N. O. (2009) *Am. J. Respir. Cell Mol. Biol.* **41**, 332–338
- Rockey, D. C., Boyles, J. K., Gabbiani, G., and Friedman, S. L. (1992) *J. Submicrosc. Cytol. Pathol.* **24**, 193–203
- Brenner, D. A., Waterboer, T., Choi, S. K., Lindquist, J. N., Stefanovic, B., Burchardt, E., Yamauchi, M., Gillan, A., and Rippe, R. A. (2000) *J. Hepatol.* **32**, (Suppl. 1) 32–38
- Shi, Z., Wakil, A. E., and Rockey, D. C. (1997) *Proc. Natl. Acad. Sci. U.S.A.* **94**, 10663–10668
- Belaguli, N. S., Schildmeyer, L. A., and Schwartz, R. J. (1997) *J. Biol. Chem.* **272**, 18222–18231
- Shao, R., Shi, Z., Gotwals, P. J., Koteliensky, V. E., George, J., and Rockey, D. C. (2003) *Mol. Biol. Cell.* **14**, 2327–2341
- Meeson, A. P., Shi, X., Alexander, M. S., Williams, R. S., Allen, R. E., Jiang, N., Adham, I. M., Goetsch, S. C., Hammer, R. E., and Garry, D. J. (2007) *EMBO J.* **26**, 1902–1912
- Mizzen, C. A., and Allis, C. D. (1998) *Cell. Mol. Life. Sci.* **54**, 6–20
- Horvai, A. E., Xu, L., Korzus, E., Brard, G., Kalafus, D., Mullen, T. M., Rose, D. W., Rosenfeld, M. G., and Glass, C. K. (1997) *Proc. Natl. Acad. Sci. U.S.A.* **94**, 1074–1079
- Tau, G., and Rothman, P. (1999) *Allergy* **54**, 1233–1251
- Darnell, J. E., Jr., Kerr, I. M., and Stark, G. R. (1994) *Science* **264**, 1415–1421
- Garneau, N. L., Wilusz, J., and Wilusz, C. J. (2007) *Nat. Rev. Mol. Cell. Biol.* **8**, 113–126
- Bisbal, C., and Silverman, R. H. (2007) *Biochimie* **89**, 789–798
- Khabar, K. S., Siddiqui, Y. M., al-Zoghbi, F., al-Haj, L., Dhalla, M., Zhou, A., Dong, B., Whitmore, M., Paranjape, J., Al-Ahdal, M. N., Al-Mohanna, F., Williams, B. R., and Silverman, R. H. (2003) *J. Biol. Chem.* **278**, 20124–20132
- Bisbal, C., Silhol, M., Laubenthal, H., Kaluza, T., Carnac, G., Milligan, L., Le Roy, F., and Salehzada, T. (2000) *Mol. Cell. Biol.* **20**, 4959–4969
- Fujita, T., Maesawa, C., Oikawa, K., Nitta, H., Wakabayashi, G., and Masuda, T. (2006) *Int. J. Mol. Med.* **17**, 605–616
- Muir, A. J., Sylvestre, P. B., and Rockey, D. C. (2006) *J. Viral Hepat.* **13**, 322–328
- Raghu, G., Brown, K. K., Bradford, W. Z., Starko, K., Noble, P. W., Schwartz, D. A., and King, T. E., Jr. (2004) *N. Engl. J. Med.* **350**, 125–133
- Friedman, S. L. (2008) *Gastroenterology* **134**, 1655–1669
- Higashi, K., Inagaki, Y., Suzuki, N., Mitsui, S., Mauviel, A., Kaneko, H., and Nakatsuka, I. (2003) *J. Biol. Chem.* **278**, 5156–5162
- Meraz, M. A., White, J. M., Sheehan, K. C., Bach, E. A., Rodig, S. J., Dighe, A. S., Kaplan, D. H., Riley, J. K., Greenlund, A. C., Campbell, D., Carver-Moore, K., DuBois, R. N., Clark, R., Aguet, M., and Schreiber, R. D. (1996) *Cell* **84**, 431–442
- Wang, D., Chang, P. S., Wang, Z., Sutherland, L., Richardson, J. A., Small, E., Krieg, P. A., and Olson, E. N. (2001) *Cell* **105**, 851–862
- Liang, S. L., Quirk, D., and Zhou, A. (2006) *IUBMB Life* **58**, 508–514
- Player, M. R., and Torrence, P. F. (1998) *Pharmacol. Ther.* **78**, 55–113
- Medjokane, S., Perez-Sanchez, C., Gaggioli, C., Sahai, E., and Treisman, R. (2009) *Nat. Cell. Biol.* **11**, 257–268